

# Doping-driven Transition to a Time-Reversal Breaking State in the Phase Diagram of the Cuprates

G. Sangiovanni, M. Capone, S. Caprara, C. Castellani, C. Di Castro, and M. Grilli

*Dipartimento di Fisica, Università di Roma "La Sapienza",*

*and Istituto Nazionale per la Fisica della Materia (INFM),*

*SMC and Unità Roma 1, Piazzale Aldo Moro 2, I-00185 Roma, Italy\**

(Dated: November 23, 2018)

Motivated by recent tunnelling and Andreev-reflection experiments, we study the conditions for a quantum transition within the superconducting phase of the cuprates, in which a bulk imaginary (time-reversal breaking)  $id_{xy}$  component appears in addition to the  $d_{x^2-y^2}$  order parameter.

We examine in detail the role of some important physical features of the cuprates. In particular we show that a closed Fermi surface, a bilayer splitting, an orthorhombic distortion, and the proximity to a quantum critical point around optimal doping favor the appearance of the imaginary component. These findings could explain why the mixed  $d_{x^2-y^2} + id_{xy}$  order parameter is observed in YBCO and LSCO, and suggest that it could appear also in Bi2212. We also predict that, in all cuprates, the mixed state should be stable only in a limited doping region all contained beneath the  $d_{x^2-y^2}$  dome. The behavior of the specific heat at the secondary transition is discussed.

PACS numbers: 74.30.Rp, 74.20.Fg, 74.25.Dw

## I. INTRODUCTION

The evidence for a  $d_{x^2-y^2}$  symmetry of the superconducting pairing in the High- $T_c$  Cuprate Superconductors (HTCS) is nowadays overwhelming<sup>1</sup>. Nonetheless it is well known that a secondary gap component of different symmetry can develop either spontaneously or driven by external factors, like a magnetic field, magnetic impurities as well as the proximity to an interface<sup>2,3,4,5</sup>. The first important consequence is that the nodal lines of the gap located along the diagonals of the Brillouin zone ( $\Gamma X$  direction) can be removed, deeply altering the low energy properties. Secondly, this kind of superconducting state can break the time-reversal symmetry with important consequences on the physical properties<sup>6</sup>. Specifically a superconducting state with mixed  $d_{x^2-y^2} + id_{xy}$  symmetry has been invoked in Refs.<sup>2,3,7</sup> to explain the thermal conductivity anomalies in  $\text{Bi}_2\text{Sr}_2\text{CaCu}_2\text{O}_8$  (Bi2212)<sup>8,9</sup>, in Ref.<sup>10</sup> to account for the properties of single quasiparticle states observed in the vortex core<sup>11</sup>, and in Ref.<sup>12</sup> as a possible explanation of the momentum and temperature dependence of the damping of quasiparticles. Scanning tunnelling experiments in  $\text{Y}_{1-y}\text{Ca}_y\text{Ba}_2\text{Cu}_3\text{O}_{7-x}$  (YBCO)<sup>13,14</sup> and in  $\text{La}_{2-x}\text{Sr}_x\text{CuO}_4$  (LSCO)<sup>15</sup> have also shown clear deviations from the pure  $d_{x^2-y^2}$ -wave symmetry. While the LSCO results have been originally interpreted in terms of a  $d + s$  wave, a recent reanalysis based on the results of the present report has shown that the  $d_{x^2-y^2} + id_{xy}$  symmetry is a more faithful description of the experiments<sup>16</sup>.

Our main motivation comes indeed from tunnelling experiment on YBCO films<sup>14</sup>, which have evidenced that the zero-bias conductance peak associated with a pure  $d_{x^2-y^2}$  gap function<sup>17</sup> undergoes a *doping- and magnetic-field-dependent* splitting. This can be interpreted<sup>18</sup> in terms of a secondary time-reversal breaking component of the superconducting gap. It is quite important to no-

tice that the amplitude of the splitting has a power-law dependence on doping and magnetic-field. The (zero-field) splitting is in fact linear in the deviation from the optimal doping for overdoped samples, and it is zero for underdoped samples. Moreover, starting from a finite (zero) value at zero field, the splitting increases linearly in the overdoped (underdoped) materials with the magnetic field, while it displays a square-root dependence close to optimal doping. These power-law dependencies are strong indications of a critical behavior due to a second-order phase transition and are hardly accounted for by surface or disorder effects alone. The above result suggests therefore a doping-driven *bulk* transition. The observed fraction of  $d_{xy}$  pairing increases with  $\delta$ , but it must be noticed that it never exceeds the 20% of the principal one in all the measured samples<sup>14</sup>. These experimental situation leaves the door open for at least two scenarios. In the first one, discussed in a different context in Ref.<sup>19</sup>, the  $d_{xy}$  component keeps increasing by further doping and eventually the gap becomes of pure  $d_{xy}$  symmetry. In the alternative scenario, which is supported by our analysis, the  $d_{xy}$  fraction does not monotonically increase, but it starts to decrease at some doping, leading to a smaller dome beneath the  $d_{x^2-y^2}$ , where the mixed order parameter is stable. Our scenario is also consistent with other experiments which put severe upper bounds for any imaginary component of the gap (see Ref.<sup>1</sup> for a recent discussion).

The experimental framework described above suggested us to carry out a systematic analysis of the specific properties which may favor the occurrence of a mixed superconducting state in some cuprates and not in others. To achieve this goal, we quantitatively analyze the role of band-structure effects (Van Hove singularity (VHS), bilayer splitting, and orthorhombic distortion), and of the form of the pairing interaction in determining the weight of the secondary component (if any), the features of the

phase diagram and the behavior of observables like the specific heat. We rely on the simple BCS approach to make the role of the above ingredients more transparent. We notice that the fact that the  $d_{x^2-y^2} + id_{xy}$  order parameter, when observed<sup>14</sup>, establishes in the overdoped regime, where strong correlation effects are less important.

In Sec. II we introduce the formalism and discuss in different subsections the effects of the Fermi surface (A), the bilayer splitting (B), the orthorhombic distortion (C) and of a QCP (D). In Sec. III we discuss how a phase diagram for the secondary component can be drawn, and Sec. IV is devoted to the conclusions.

## II. METHOD AND RESULTS

General theoretical constraints for the appearance of a bulk mixed order parameter have already been studied, e.g., in Refs.<sup>5,20</sup>. In particular, in the first of these works it has been shown that the mixed state is more likely to establish close to a surface than in the bulk and that the  $id_{xy}$  wave is the most favored secondary component in both cases.

Here we recall some basic symmetry arguments and derive the BCS equations. The strong anisotropy of the HTCS allows us to focus on a purely two-dimensional lattice system, characterized by the  $C_{4v}$  point group. Only the four harmonics corresponding to the one-dimensional irreducible representations of the group are compatible with singlet pairing. We can write them as<sup>21</sup>

$$\begin{aligned} w_{\mathbf{r};\mathbf{k}}^{s^+} &= \cos k_x x \cos k_y y + \cos k_x y \cos k_y x, \\ w_{\mathbf{r};\mathbf{k}}^{s^-} &= -\sin k_x x \sin k_y y + \sin k_x y \sin k_y x, \\ w_{\mathbf{r};\mathbf{k}}^{d^+} &= \cos k_x x \cos k_y y - \cos k_x y \cos k_y x, \\ w_{\mathbf{r};\mathbf{k}}^{d^-} &= -\sin k_x x \sin k_y y - \sin k_x y \sin k_y x. \end{aligned}$$

Then, the gap function can be written as

$$\Delta_{\mathbf{k}} = \sum_{\eta} \Delta_{\mathbf{k}}^{\eta} = \sum_{\eta} \sum_{\mathbf{r}}' \Delta_{\mathbf{r}}^{\eta} w_{\mathbf{r};\mathbf{k}}^{\eta}, \quad (1)$$

where the index  $\eta = s^+, s^-, d^+, d^-$  labels the different representations and  $\mathbf{r} = (x, y)$ , with integer  $x, y$ , denotes a lattice site (we take the lattice spacing  $a_x = a_y = 1$ ). The primed sum is restricted to inequivalent sites under the symmetry of the lattice (i.e., to the different lattice distances). If we require the invariance of  $|\Delta_{\mathbf{k}}|^2$  under the point group transformations, the gap function has to transform either like a single representation, or like a complex (time-reversal breaking) combination of the form  $\Delta_{\mathbf{k}}^{\eta} + i\Delta_{\mathbf{k}}^{\zeta}$  with  $\eta \neq \zeta$ .

Expanding the BCS equation in the same harmonics, it is easy to realize that the appearance of a harmonic labeled by  $\mathbf{r}$  is controlled by the correspondent component of the pair potential  $V(\mathbf{r})$ . In a generic model for

the cuprates the on-site interaction ( $V_0$ ) is repulsive (positive) due to strong local repulsion. The longer distance part ( $V_{i \neq 0}$ ) is instead attractive (negative) and it is reasonably assumed to be a decreasing function of distance. We can therefore restrict to the smallest distance harmonics. In the following we always use the symbol  $V_i$  to denote the modulus of the  $V(\mathbf{r} = \mathbf{i})$ . For  $\mathbf{r} = 0$ , the only nonzero harmonic belongs to the  $s^+$  representation, and corresponds to the isotropic  $s$ -wave, which is ruled out by the repulsive  $V_0$ . For  $\mathbf{r} = (\pm 1, 0); (0, \pm 1) \equiv \mathbf{1}$  the  $s^+$  and  $d^+$  representations are associated with the extended  $s_{x^2+y^2}$  and  $d_{x^2-y^2}$  waves, respectively. For  $\mathbf{r} = (\pm 1, \pm 1) \equiv \mathbf{2}$ , the non-vanishing harmonics are related to the  $s_{xy}$  and  $d_{xy}$  waves ( $s^+$  and  $d^-$  representations).

If we take a complex combination of the form  $\Delta_1 w_{\mathbf{1};\mathbf{k}}^{\eta} + i\Delta_2 w_{\mathbf{2};\mathbf{k}}^{\zeta}$ , with both  $\Delta_1$  and  $\Delta_2$  real, each gap parameter affects the other only through the quasiparticle spectrum and the secondary pairing can be viewed as a BCS coupling between the Bogoljubov quasiparticles of the primary superconducting phase. The BCS equations then read

$$\frac{1}{V_1} = \int \frac{d\mathbf{k}}{4\pi^2} \left( w_{\mathbf{1};\mathbf{k}}^{\eta} \right)^2 \frac{\tanh(\beta E_{\mathbf{k}}/2)}{2E_{\mathbf{k}}} \equiv I_1 \quad (2)$$

$$\frac{1}{V_2} = \int \frac{d\mathbf{k}}{4\pi^2} \left( w_{\mathbf{2};\mathbf{k}}^{\zeta} \right)^2 \frac{\tanh(\beta E_{\mathbf{k}}/2)}{2E_{\mathbf{k}}} \equiv I_2 \quad (3)$$

where  $\beta$  is the inverse temperature,  $E_{\mathbf{k}} = [\xi_{\mathbf{k}}^2 + (\Delta_1 w_{\mathbf{1};\mathbf{k}}^{\eta})^2 + (\Delta_2 w_{\mathbf{2};\mathbf{k}}^{\zeta})^2]^{1/2}$ , with  $\eta = s^+, d^+$ ,  $\zeta = s^+, d^-$  ( $\eta \neq \zeta$ ). The band dispersion is  $\xi_{\mathbf{k}} = -2t(\cos k_x + \cos k_y) + 4t' \cos k_x \cos k_y - \mu$  where  $t$  and  $t'$  are nearest and next-nearest neighbor hoppings and  $\mu$  is the chemical potential. Density functional theory gives a typical value for the hopping  $t$  in the HTCS of 200 meV, while  $t'$  assumes different values in the various compounds<sup>22</sup>. These values can however be reduced by a factor of two by correlation effects, that can be estimated by fitting the angular resolved photoemission spectra with a tight-binding model. As we will see later in more detail, the value of  $t'$  has important effect on the DOS, since it controls the position of the Van Hove singularity (VHS).

Being the largest attractive coupling  $V_1$  controls the principal component of the gap, which can be  $d_{x^2-y^2}$  or  $s_{x^2+y^2}$ . For typical values of the particle density in the HTCS, both low doping and the VHS of the two-dimensional DOS strongly favor the  $d_{x^2-y^2}$  symmetry, which thus represents the principal component of the superconducting gap even in the simplified BCS approach<sup>23</sup>. We take henceforth  $\eta = d^+$  in Eqs. (2),(3). The spectrum for the secondary  $\zeta$  component is therefore (pseudo)gapped by the principal  $d_{x^2-y^2}$  gap  $\Delta_1$ . As a consequence, the mixed order parameter establishes only for  $V_2$  larger than a critical value  $V_2^{cr}$ , as opposed to the case of the Cooper instability in the metallic phase, which takes place for arbitrarily small coupling. The critical coupling for both  $d_{xy}$  and  $s_{xy}$  secondary pairing is determined by solving the BCS equations (2),(3) with  $\Delta_2 = 0$

and  $\zeta = d^-, s^+$  respectively. The only difference between these two cases is the different form of the harmonic  $w_{\mathbf{2};\mathbf{k}}^{\zeta}$  that weights the same kernel in  $I_2$ . This kernel, in turn, is affected by the presence of the  $d_{x^2-y^2}$  wave. The  $d_{x^2-y^2}$  gap in the  $E_{\mathbf{k}}$  spectrum strongly suppresses the contributions from the M points  $(0, \pm\pi), (\pm\pi, 0)$ , while it does not affect much the nodal lines. The  $d_{xy}$  wave has nodes along the  $\Gamma\text{M}$  directions and is maximum along the diagonals, while the  $s_{xy}$  has its maximum contributions from the M points, just like the  $d_{x^2-y^2}$ . It is therefore clear that the  $d_{xy}$  is most likely candidate for the secondary component<sup>5</sup>.

A numerical solution of the above Eqs. (2),(3) confirms the above arguments, finding  $V_2^{cr}$  always larger for  $s_{xy}$  than for  $d_{xy}$ . Moreover, the appearance of the  $s_{xy}$  component is generally associated to a first-order transition from pure  $d_{x^2-y^2}$  to pure  $s_{xy}$ , since the continuous mixing is unlikely due to the strong competition between the two harmonics. This kind of scenario is clearly incompatible with the experiments, in which the secondary component appears in a continuous way. The continuous transition from  $d_{x^2-y^2}$  to  $d_{x^2-y^2} + id_{xy}$  gap is therefore the most natural candidate if a pure  $d_{x^2-y^2}$  is to be modified by a small secondary component, as suggested by the experiments on YBCO<sup>14</sup> and on LSCO<sup>15</sup>.

Next, we evaluate the critical value of  $V_2$  to get  $d_{xy}$  pairing,  $V_{d_{xy}}^{cr} \equiv V^{cr}$ , assuming a given value of  $V_1$ . A similar analysis has been performed in Ref.<sup>5</sup> for a continuous model, and in Ref.<sup>20</sup> for a lattice model. In the latter case, in which the effect of a two-dimensional DOS is considered, it is always found that  $V^{cr} > V_1$ . This would imply that a secondary component is possible only taking a potential which increases with the distance, at least going from nearest to next-nearest neighbors. This condition seems hard to be realized in a microscopic model, where the interaction is naturally a decreasing function of distance. Similar results have been obtained also within a  $t$ - $J_1$ - $J_2$  model in<sup>19</sup>, where the  $d_{x^2-y^2} + id_{xy}$  and pure  $d_{xy}$  establish, respectively, for  $J_2/J_1 \simeq 1.4$  and 2.2, which are clearly not representative of the cuprates. In the case of Ref.<sup>5</sup>,  $V^{cr}/V_1$  may be smaller than one for some values of the parameters, but this only comes from the assumption of a flat DOS, which is clearly not representative of the HTCS.

Having in mind that for a plausible microscopic potential  $V_2 < V_1$ , in the following we explore the conditions for the appearance of the secondary harmonic obeying this constraint. First we notice that the larger is the value of  $V_1$  is, the smaller is the ratio  $V^{cr}/V_1$ . In other words, if both the couplings are large, a secondary component may appear also for  $V_2 < V_1$ . The above claim can be understood as follows: If we increase  $V_1$ ,  $\Delta_1$  also increases, and it has different effects on the two equations. The integral  $I_2$  in Eq. (3) does not change much by increasing  $\Delta_1$ , due to the  $w_{\mathbf{2};\mathbf{k}}^d$  factor, while  $I_1$  instead contains  $w_{\mathbf{1};\mathbf{k}}^d$ , and it is therefore substantially reduced by  $\Delta_1$ . Since, from Eqs. (2),(3),  $V^{cr}/V_1 = I_1/I_2$ , this implies that, at fixed band dispersion, the larger is  $V_1$ , the smaller is the

ratio  $V^{cr}/V_1$  and then the mixed state is more favored.

The argument above shows that strong coupling is necessary for the appearance of a secondary component<sup>24</sup>. Nevertheless,  $V_1$  can not be increased indefinitely without pushing the value of  $\Delta_1$  to unphysical values. If we want to increase the  $d_{x^2-y^2}$ -coupling at fixed  $\Delta_1$  we can introduce a cut-off  $\omega_0$  in the integrals. This cut-off is not just an artifact to push the system to stronger coupling, but naturally measures the typical energy scale of the attractive potential. In the forthcoming calculations we take  $\omega_0 = 50 \text{ meV} = 0.25t$ .<sup>25</sup> As we see in the following, this choice of cut-off leads us to reasonable phase diagrams without assuming unphysical values of the gap.

Now we discuss the role of different physical effects on the value of the critical  $V_2$ . Some preliminary considerations may be done before numerically solving the BCS equations. In a BCS approach, the bandstructure influences the values of the gap and of the critical temperature only through the DOS. In particular, the VHS plays the main role, strongly favoring the pure  $d_{x^2-y^2}$  pairing. Other harmonics may be stabilized only for doping values for which the chemical potential is sufficiently far from the VHS. This means that, if we want the  $d_{xy}$  to appear for dopings, like the ones of the experiments, the VHS must be relatively close to half-filling. This is realized for cuprates with closed Fermi surface like LSCO. To explain the appearance of the secondary component in YBCO we therefore have to invoke some other effects, like orthorhombic distortion or bilayer splitting. Both this effects are expected to help the secondary component to appear, because they “regularize” the VHS. We discuss the role of these effects in the following subsections. The final subsection is instead dedicated to the form of the pairing potential  $V(\mathbf{r})$ , and in particular to the possible role of a QCP in the charge sector close to optimal doping<sup>26</sup>.

### A. Shape of the Fermi Surface

As we mentioned above, the position of the VHS plays an important role in determining the symmetry of the order parameter within the BCS approach. The ratio  $t'/t$  is a direct measure of the position of the VHS, and consequently of the shape of the Fermi surface. For  $t' = 0$ , the VHS lies at the chemical potential at half-filling. Increasing  $t'/t$ , the density for which the chemical potential lies at the VHS moves away from half-filling. Consequently, the stability of the pure  $d_{x^2-y^2}$  wave extends to larger doping, making the appearance of the  $d_{xy}$  more difficult. We numerically solve Eqs. (2) and (3) to make the analysis more quantitative. The results are reported in Fig. 1. Here we take  $V_1$  constant as a function of doping, just to avoid the complications of many varying parameters and to disentangle the effect of the VHS. It is understood that  $V_1$  will depend on doping in a realistic description of the cuprates.

According to the discussion above ( $V_2 < V_1$ ), the sec-

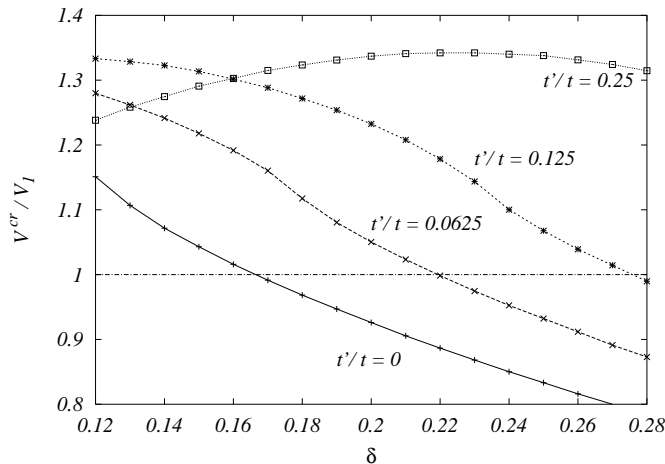


FIG. 1:  $V^{cr}/V_1$  as a function of the doping  $\delta$  for  $V_1/t = 1.15$ ,  $\omega_0/t = 0.25$  and different values of the ratio  $t'/t$ . When the curve crosses the line  $V^{cr}/V_1 = 1$  the appearance of the secondary harmonics becomes possible with  $V_2 < V_1$ .

ondary harmonics can only appear, roughly speaking, when  $V^{cr}/V_1 < 1$ . The appearance of the secondary harmonic is more likely as the doping increases, but the minimal doping  $\delta_{min}$  above which  $V^{cr}/V_1 < 1$  increases with  $t'/t$ .  $\delta_{min}$  assumes values compatible with the experimental findings only for (small) values of  $t'/t$  such that the Fermi surface is closed, while an open Fermi surface pushes  $\delta_{min}$  to exceedingly large values. This analysis suggests that the  $d_{x^2-y^2} + id_{xy}$  pairing may likely occur in LSCO, where the Fermi surface is expected to be closed, at least in the optimal and overdoped region. Other physical effects must be invoked for open Fermi surface materials like YBCO or Bi2212.

### B. Bilayer Splitting

Materials like YBCO and Bi2212 have relatively large values  $t'/t \gtrsim 0.25$ , and therefore open Fermi surfaces, which favor, according to the previous analysis, a pure  $d_{x^2-y^2}$  pairing. However, the strict two-dimensionality assumed up to now overestimates the effect of the VHS, which strongly favors the  $d_{x^2-y^2}$  wave. YBCO and Bi2212, as opposed to LSCO, are indeed multi-layer cuprates. Introducing the multi-layer structure of Bi2212 and YBCO results in a “regularization” of the VHS. ARPES measurements in Bi2212 show indeed a bilayer splitting  $2t_\perp$  at the M points which, although smaller than the one predicted by band-structure calculations<sup>22</sup>, is sizable, and varies from 88 meV to 140 meV<sup>27</sup>. We are not aware of similar data on YBCO (where ARPES measurements are much harder to perform), but the bare values of  $t_\perp$  in Bi2212 and YBCO are similar, so that we can expect similar renormalized values.

To analyse the role of a bilayer structure we introduce

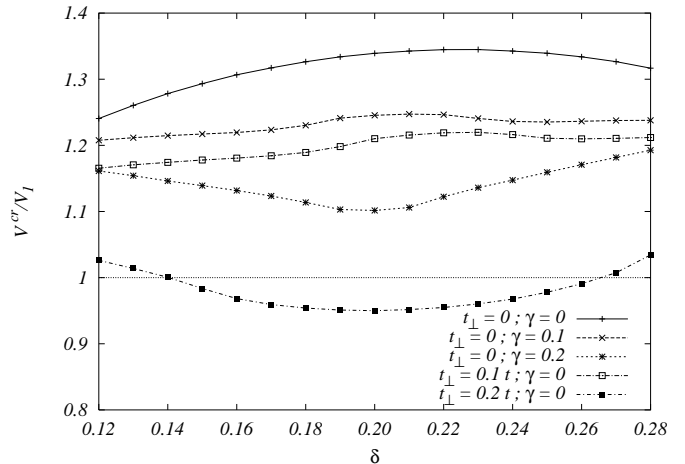


FIG. 2:  $V^{cr}/V_1$  as a function of the doping  $\delta$  for  $V_1/t = 1.15$ ,  $\omega_0/t = 0.25$  and different values of the splitting parameter  $t_\perp$  and of the orthorhombic parameter  $\gamma = (t_y - t_x)/t_x$ . The upper curve is the same as that shown in Fig.1.

a band splitting of the form  $\frac{1}{2}t_\perp(\cos k_x - \cos k_y)^2$  which modifies the effective DOS and splits the VHS partially spoiling the  $d_{x^2-y^2}$  principal component. On the other hand, the nodal regions are not affected and so one expects the ratio  $V^{cr}/V_1$  to decrease as soon as  $t_\perp \neq 0$ . In Fig.2 we show the doping dependence of  $V^{cr}/V_1$  for the same values of  $V_1$  and of  $\omega_0$  as in the case of Fig.1. The two curves with open and solid squares corresponds to the case  $t_\perp = 0.1t$  and  $0.2t$  respectively and are, as expected, lower than that for  $t_\perp = 0$ . As can be seen in the figure, the second of these curves, which still compatible with the measured value of  $t_\perp$  is Bi2212, has been lowered enough to cross the  $V^{cr}/V_1 = 1$  line.

In conclusion, the bilayer splitting helps the  $d_{xy}$  component to establish at least in all those doping regions for which the chemical potential falls in the dip of the density of states centered at  $-4t'$ , leaving one of the two Fermi surfaces open. This is a relevant scenario for the case of YBCO and Bi2212 in which the Fermi surfaces is open.

### C. Orthorhombic Distortion

Another important effect that lowers the impact of the VHS on the pairing in the cuprates is an orthorhombic splitting of the bands. This is accounted for by taking a dispersion of the form  $\xi_{\mathbf{k}} = -2(t_x \cos k_x + t_y \cos k_y) + 4t' \cos k_x \cos k_y - \mu$  and  $t_x \neq t_y$ . In this way  $\xi_{\mathbf{k}}$  and the kernel containing  $E_{\mathbf{k}} = [\xi_{\mathbf{k}}^2 + |\Delta_{\mathbf{k}}|^2]^{1/2}$  that enters the equations (2),(3), are no longer symmetric functions with respect to the  $C_{4v}$  group. In any case this kernel can still be expanded in terms of the  $C_{4v}$ -harmonics and one can solve the resulting coupled equations. However, if the orthorhombic distortion is small, one can neglect the effects

on the symmetry of the gap and take only the larger effects on the density of states. In doing this, one neglects the  $d^+-s^+$  and  $d^--s^-$  mixing that arises because the  $\mathcal{C}_{4v}$ -group symmetry of the system has been lowered to  $\mathcal{C}_{2v}$ . In fact, the basis functions for the two one-dimensional representations of  $\mathcal{C}_{2v}$  that couples to the singlet are given by  $w_{\mathbf{r};\mathbf{k}}^{s^+} + w_{\mathbf{r};\mathbf{k}}^{d^+}$  respectively, and what we do in the following is to project our solutions on the original  $d_{x^2-y^2}$  and  $d_{xy}$  harmonics in order to understand the role of a small orthorhombic distortion on the  $d_{x^2-y^2} + id_{xy}$  solution.

The density of states is then qualitatively similar to the bilayered one. In fact the VHS is split and one expects that when the chemical potential lies in the dip the secondary  $d_{xy}$  component is again favored with respect to the case with  $t_x = t_y$ . The results are represented by the two curves with crosses and stars in Fig.2. We have used for  $t_x$  the same value of 200 meV as before for  $t$  and varied the ratio  $(t_y - t_x)/t_x$  denoted as  $\gamma$ .  $V_1$  and  $\omega_0$  are still those of the Fig.1. In the case of  $\gamma = 0.1$  (crosses) the ratio  $V^{cr}/V_1$ , although lower than for the isotropic one, is still greater than 1, as well as that for  $\gamma = 0.2$  (stars) even if in this last one the characteristic upward curvature coming from the presence of the dip in the DOS can be clearly seen. As for the bilayer case we have used a constant value for  $V_1$  aiming at analysing the effects of band structure of the orthorhombic distorted compounds on the critical coupling, and we have evidenced that the  $d_{xy}$  secondary component is favored by this effect. The values of  $\gamma$  that we have used are representative of the case of the cuprates according to, e.g., Ref.<sup>28</sup> where a value of  $\gamma \sim 0.1$  is found by means of *ab-initio* calculations for the case of LSCO.

#### D. Quantum Criticality around Optimal doping

We now discuss how the form of the pair potential can be important to obtain the  $d_{x^2-y^2} + id_{xy}$  order parameter. In particular, we discuss how this phenomenology can be related to the QCP scenarios for HTCS<sup>29,30,31</sup>. In this context, it has been suggested that the pairing may be mediated by quasi-critical fluctuations close to the QCP in the charge and/or spin sector(s) located near optimal doping. In this framework the correlation function of the critical fluctuations determines the functional form of the pairing potential. A few different QCP have been proposed, ranging from magnetic and/or charge ordering, to time reversal breaking. In the last part of this section we briefly discuss the case of charge and spin ordering, while here we first discuss some general consequences of a QCP near optimal doping which are independent on the nature of the ordered phase. Far from criticality (i.e., far from optimal doping) the short-range components  $V_1, V_2, \dots$  may decrease strongly with the distance. At criticality the correlation saturates below a non-universal length scale, and all the components of the potential below this scale become of the same order of magnitude.  $V_2$  then becomes of the order of  $V_1$ , favoring the appearance of

a secondary component of the gap. This establishes the connection between the  $d_{x^2-y^2} \rightarrow d_{x^2-y^2} + id_{xy}$  transition and the underlying quantum criticality. One may notice that, close to the QCP, where various couplings are of the same order of magnitude, higher-order harmonics should in principle be considered within each irreducible representation. The main outcome of this extension would only be a more detailed description of the gap profile, without changing the symmetry of the order parameter. Observed deviations from a pure  $d_{x^2-y^2}$  gap can be explained in this context<sup>32</sup>.

We now consider the specific case of a pairing interaction mediated by the fluctuations around a charge ordering QCP, with an incommensurate ordering vector  $\mathbf{Q} = (Q_x, Q_y)$ . The effective interaction between quasi-particles in the Cooper channel can be written as

$$V_{\mathbf{k}-\mathbf{k}'} = U - \frac{1}{8} \sum_{\alpha} \frac{V_c}{\kappa^2 + \omega_{\mathbf{k}\mathbf{k}'}(\mathbf{Q}^{\alpha})}, \quad (4)$$

where  $U$  is a residual local repulsion,  $V_c$  is the attraction strength,  $\kappa^2$  is a “mass term” measuring the distance from criticality, and  $\omega_{\mathbf{k}\mathbf{k}'}(\mathbf{Q}^{\alpha}) = 2(2 - \cos(k_x - k'_x - Q_x^{\alpha}) - \cos(k_y - k'_y - Q_y^{\alpha}))$  contains the momentum dependence of the interaction. The sum over the eight momenta  $\mathbf{Q}^{\alpha} = (\pm Q_x, \pm Q_y), (\pm Q_y, \pm Q_x)$  makes the interaction symmetric under the  $\mathcal{C}_{4v}$  group.

The real-space expression for (4) is particularly useful in light of the previous analysis. We can in fact write

$$V(\mathbf{r}) = U\delta_{\mathbf{r},0} - \frac{1}{2}V_c\alpha_{\mathbf{r}}(\kappa^2)w_{\mathbf{r};\mathbf{Q}}^{s^+}. \quad (5)$$

The local repulsion obviously enter only in the on-site coupling and does not therefore play any role in the  $d_{x^2-y^2} \rightarrow d_{x^2-y^2} + id_{xy}$  transition.  $\alpha_{\mathbf{r}}(\kappa^2)$  are dimensionless functions of  $\kappa^2$  and the lattice distances  $\mathbf{r}$ . When the system is at the critical point, i.e., in the limit  $\kappa^2 \rightarrow 0$ , all the  $\alpha_{\mathbf{r}}$  approach the same value regardless of the index  $\mathbf{r}$ , as we expected from the general arguments given above. The dependence on the critical vector  $\mathbf{Q}$  is entirely contained in the symmetry factor  $w_{\mathbf{r};\mathbf{Q}}^{s^+}$ , i.e., in the above defined harmonics computed at the ordering vector  $\mathbf{Q}$ . The first two coupling constants that enter the BCS equations (2) and (3) are then given by  $V_1 = \frac{1}{2}V_c\alpha_1 w_{1;\mathbf{Q}}^{s^+} = \frac{1}{2}V_c\alpha_1(\cos Q_x + \cos Q_y)$  and  $V_2 = \frac{1}{2}V_c\alpha_2 w_{2;\mathbf{Q}}^{s^+} = V_c\alpha_2 \cos Q_x \cos Q_y$ <sup>33</sup>. The modulation of the couplings introduced by the critical momentum  $\mathbf{Q}$  determines regions in which some coupling may become repulsive, thus making the correspondent harmonic impossible to establish. In particular, the  $d_{x^2-y^2} + id_{xy}$  symmetry is possible only if both  $V_1$  and  $V_2$  are attractive, i.e., for  $Q_x \in [-\pi/2 : \pi/2]$  and  $Q_y \in [-\pi/2 : \pi/2]$ . Moreover, the ratio  $V_2/V_1$  is proportional to the form factor  $2 \cos Q_x \cos Q_y / (\cos Q_x + \cos Q_y)$ , and it is therefore maximum at  $\mathbf{Q} = (0, 0)$ . The mixed symmetry order parameter is therefore more likely for small ordering vectors.

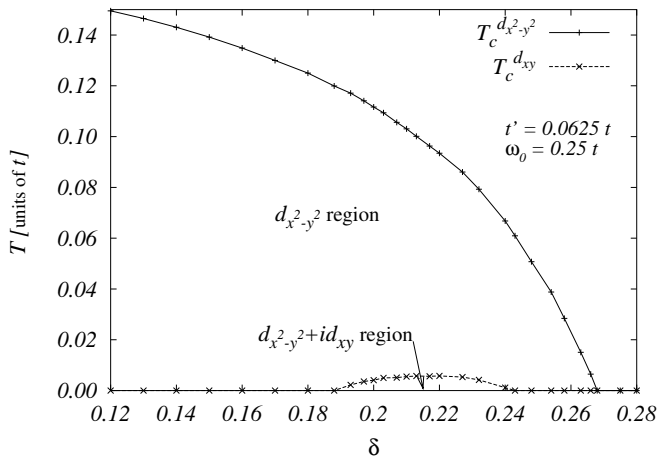


FIG. 3: Phase diagram for  $d_{x^2-y^2}$  and  $d_{x^2-y^2} + id_{xy}$  pairing in the HTCS. The parameters, which are appropriate for open Fermi surface cuprates, are given in the text.

The contribution to the pairing interaction coming from the spin sector can be written in the same way as (4), with an opposite sign. This implies that pairing mechanisms based on antiferromagnetic spin fluctuations<sup>31</sup>, with ordering vector  $\mathbf{Q} = (\pi/2, \pi/2)$  strongly favor  $d_{x^2-y^2}$  pairing, which is maximum for this vector, while the  $V_2$  coupling is repulsive for the same vector. Even taking into account small incommensurations around the antiferromagnetic vector, spin fluctuations mechanisms do not favor the appearance of the  $d_{x^2-y^2} + id_{xy}$  order parameter. Because of the relevance of antiferromagnetic spin fluctuations in the underdoped region of the phase diagram of the cuprates this analysis indicates that the mixed  $d_{x^2-y^2} + id_{xy}$  state should not be present at least in the extremely underdoped compounds, in agreement with the experiments.

To summarize the main outcome of this section, the proximity to a QCP helps in meeting the necessary conditions for the mixed symmetry (i.e., strong coupling and  $V_2/V_1$  close to 1). Nevertheless, the specific nature of the QCP (like, e.g., charge and/or spin ordering) may introduce sign modulations of the real-space interaction, making some components repulsive, and therefore suppressing the correspondent harmonics. The pairing mechanism based on antiferromagnetic spin fluctuations<sup>31</sup> strongly favors the  $d_{x^2-y^2}$  pairing, but suppresses the  $d_{xy}$  channel, leading to pure  $d_{x^2-y^2}$ . Mechanisms based on charge fluctuations support instead a secondary  $d_{xy}$  component besides a primary  $d_{x^2-y^2}$  provided the characteristic ordering wave vector  $\mathbf{Q}$  is not too large ( $|\mathbf{Q}| < \pi/2$ ).

### III. PHASE DIAGRAM

We can now draw a phase diagram for the  $d_{x^2-y^2} + id_{xy}$  pairing by fixing  $V_1$  for each doping  $\delta$ , such that the

mean field critical temperature for  $d_{x^2-y^2}$  pairing (which we interpret as the temperature for Cooper pair formation without phase coherence in the underdoped regime) grossly follows the behavior of the pseudogap temperature  $T^*$  for small values of  $\delta$ , and becomes negligibly small for the doping at which  $T_c$  vanishes in the overdoped regime. In this way we phenomenologically introduce the doping dependence of the principal component of the interaction  $V_1(\delta)$ . In particular  $V_1(\delta)$  will be larger at low doping and decrease toward weak coupling in the overdoped regime. Around optimal doping we obtain  $V_1/t \simeq 2$ , which is larger than the value we used to draw the diagrams of Figs. 1 and 2, and, according to the previous discussion on the relevance of the strong coupling, is more favorable for the  $d_{x^2-y^2} + id_{xy}$  pairing.

On the other hand, we consider the less favorable situation in terms of bandstructure by using the single-layer isotropic dispersion ( $t_{\perp} = 0$  and  $\gamma = 0$ ). According to the previous analysis, in order to have a chance to observe a  $d_{xy}$  component in this unfavorable situation, we need to assume a small value of  $t' = 0.0625t$  which gives a closed Fermi surface in the relevant doping range. The value of the interaction is obviously crucial. Here we take, at any doping,  $V_2/V_1 = 0.8$ , a relatively large value, which, as we have seen, can be reasonably reached if a QCP is located close to optimal doping. This constant value of  $V_2/V_1$  allows us to analyse the combined role of the density of states and of the doping dependence of the principal coupling. In Fig. 3, we show  $T_c$  for  $d_{x^2-y^2}$  pairing (top curve) described above, and the critical temperature for the onset of the secondary pairing (bottom curve), calculated by solving the coupled BCS equations (2) and (3). As shown in Fig. 3, the mixed  $d_{x^2-y^2} + id_{xy}$  order parameter is stabilized in a small dome slightly shifted in the overdoped region,  $0.19 < \delta < 0.24$ , and the  $d_{xy}$  gap is always only a small fraction of the  $d_{x^2-y^2}$  gap.

The shape of the mixed state region is the consequence of the balance between two main effects: *i*) the  $d_{xy}$  can establish only when the VHS is far enough from the chemical potential, and therefore appears only above a given value of the doping. *ii*) Further overdoping,  $V_1(\delta)$  decreases and pushes the system toward weak coupling, where the mixed order parameter ceases to be stable for reasonable values of  $V_2/V_1$ . The dome shape is therefore an unavoidable consequence of taking a sensible value for the ratio  $V_2/V_1 < 1$ . Only by releasing this physical condition, and taking  $V_2/V_1 \gg 1$  the  $d_{xy}$  component may indefinitely increase by overdoping, eventually leading to a pure  $d_{xy}$  pairing in the heavily overdoped region<sup>19</sup>. The re-analysis of the LSCO data<sup>15</sup> with a  $d_{x^2-y^2} + id_{xy}$  gap parameter, clearly displays the closure of the dome in the overdoped region, in qualitative agreement with our analysis.

We note that small variations of the ratio  $V_2/V_1$  can significantly modify the amplitude of the secondary component. At doping  $\delta = 0.22$ , for example, by slightly enhancing  $V_2/V_1$  from 0.8 to 0.9, the critical temperature for the  $d_{x^2-y^2} + id_{xy}$  state is enhanced by a factor

of 3.

Up to now, we have found that the  $d_{x^2-y^2} \rightarrow d_{x^2-y^2} + id_{xy}$  transition can be found for values of the parameters appropriate to the single layer isotropic case with open Fermi surface. The discussions of Sec. II B, C have shown that, as soon as small perturbations of the pure two-dimensional bandstructure are considered, the constraints for the onset of the secondary component are partially released. The data of Fig. 2 show in fact that for a realistic value of the bilayer splitting, the whole region  $0.14 < \delta < 0.26$  becomes compatible with a  $d_{x^2-y^2} + id_{xy}$  order parameter. Analogously, a small orthorhombic distortion lowers the values of the critical coupling. Once realistic bandstructure parameters involving the above effects are used, the appearance of the time-reversal breaking order parameter in LSCO and YBCO, as well as the doping dependence, can be easily explained in the simple BCS approach. The physical mechanisms leading to the mixed order parameter here presented have however a general content which does not depend explicitly on the use of the BCS approach. It is important to stress that the 'dome behavior' of the mixed order parameter does not depend on the details of the calculations, and represents a generic result within our approach.

The experimental studies which motivated our work identified the transition to the mixed  $d_{x^2-y^2} + id_{xy}$  wave with the splitting on the zero bias conductance peak. Here we finally discuss the possibility to provide a further experimental signature of the mixed order parameter by measuring the variation of the specific heat coefficient  $\gamma_{c_V} = c_V/T$  at  $d_{x^2-y^2} \rightarrow d_{x^2-y^2} + id_{xy}$  transition. For the parameters used to draw the phase diagram of Fig. 3, we have computed the mean-field jump of the specific heat at  $\delta = 0.22$ , where the secondary component is maximum, and the effect of the second transition should be more evident. We actually computed the entropy as a function of temperature, and extracted the specific heat from  $c_V = TdS/dT$ .

In this specific case, at the transition from the metal to the  $d_{x^2-y^2}$  superconductor we obtain  $\Delta\gamma_{c_V}/\gamma_{c_V} = 1.00$ . At the  $d_{x^2-y^2} + id_{xy}$  transition (which occurs approx. at 10 K in this case) we obtain instead  $\Delta\gamma_{c_V}/\gamma_{c_V} = 0.28$ . We note that the absolute value of  $\Delta\gamma_{c_V}$  in the latter case is about two orders of magnitude smaller than in the former, higher temperature transition. Even though fluctuation effects are expected to round the mean-field jump, our estimated value of  $\Delta\gamma_{c_V}$  suggests that the effect could be still experimentally detected.

#### IV. CONCLUSIONS

We have performed a systematic analysis of the possibility of a  $d_{x^2-y^2} + id_{xy}$  symmetry pairing in the cuprates

by means of the simple BCS approach which is indeed justified by the experimental evidence that the mixed order parameter establishes in the overdoped region. Our results are compatible with all the available indications of  $d_{x^2-y^2} + id_{xy}$  pairing in YBCO and LSCO. We have separately discussed the role of the bandstructure effects and of the pairing potential. Since the VHS is an obstacle to the mixed pairing, all the effects that lower the impact of the singularity result in an enhanced tendency toward the  $d_{x^2-y^2} + id_{xy}$  pairing. In particular, the bilayer splitting characteristic of multilayer cuprates and the orthorhombic splitting of the bands both favor the mixed order parameter. The relevance of the bilayer splitting suggests that, Bi2212 is also likely to show a mixed order parameter, with a small mixing of the same order of YBCO.

As far as the pairing potential is concerned, we have shown that a mixed-symmetry superconducting state is more likely to establish at strong coupling. In particular, it can appear for  $V_2/V_1 < 1$  only at strong coupling. The presence of a QCP around optimal doping is an important ingredient, since it enhances the coupling and makes the next-nearest neighbor component of the pairing potential (responsible for the  $d_{xy}$  pairing) of the same order of the nearest neighbor one (responsible for  $d_{x^2-y^2}$ ).

The main result of our analysis is that a mixed order parameter of the form  $d_{x^2-y^2} + id_{xy}$  can be stabilized in a small dome contained in the larger  $d_{x^2-y^2}$  region with a pairing potential being a decreasing function of the distance, i.e.,  $V_2 < V_1$ . Contrary to other scenarios, the  $d_{xy}$  component does not grow indefinitely with increasing doping and it is always smaller than the  $d_{x^2-y^2}$ . The only way to obtain an indefinitely increasing  $d_{xy}$  component is to take an unphysically large ratio  $V_2/V_1 \gg 1$ .

We have also shown that  $d_{x^2-y^2} + id_{xy}$  pairing is more likely to occur for materials with closed Fermi surfaces such as LSCO, and in compounds where an inter-layer hopping splits the VHS. The less important role of the VHS in the electron-doped materials may lead to the  $d_{x^2-y^2} + id_{xy}$  state also in these family of compounds. We have also discussed the impact of the secondary transition on specific heat measurements, showing that the relative jump of the linear specific heat coefficient is a fraction of the jump at the primary (higher temperature) transition to the  $d_{x^2-y^2}$  superconducting phase.

\*\*\*

We thank D. Daghero, R.S. Gonnelli and G.A. Ummarino for useful discussions and for having shown us the reanalysis of their data prior to publication. Discussions with A. Toschi are also acknowledged. We acknowledge financial support by MIUR Cofin 2001, prot. 2001023848, and by INFN/G (through PA-G0-4).

\* Electronic address: massimo.capone@roma1.infn.it

<sup>1</sup> C. Tsuei and J. Kirtley, Rev. Mod. Phys. **72**, 969 (2000).

- <sup>2</sup> R.B. Laughlin, Phys. Rev. Lett. **80**, 5188 (1998).
- <sup>3</sup> A. V. Balatsky, Phys. Rev. Lett. **80**, 1972 (1998).
- <sup>4</sup> L. J. Buchholtz *et al.*, J. Low Temp. Phys. **101**, 1079 (1995).
- <sup>5</sup> M. Matsumoto and H. Shiba, J. Phys. Soc. Jpn. **64**, 3384 (1995).
- <sup>6</sup> M. Sigrist, Prog. Theor. Phys. **99**, 899 (1998).
- <sup>7</sup> H. Ghosh, Europhys. Lett. **43**, 707 (1998).
- <sup>8</sup> K. Krishana *et al.*, Science **277**, 83 (1997).
- <sup>9</sup> R. Movshovich *et al.*, Phys. Rev. Lett. **80**, 1968 (1998).
- <sup>10</sup> M. Franz and Z. Tešanović, Phys. Rev. Lett. **80**, 4763 (1998).
- <sup>11</sup> I. Maggio-Aprile *et al.*, Phys. Rev. Lett. **75**, 2754 (1995); S. H. Pan *et al.*, *ibid.* **85**, 1536 (2000); B. W. Hoogenboom *et al.*, *ibid.* **87**, 267001 (2001).
- <sup>12</sup> M. Vojta, Y. Zhang, S. Sachdev, Phys. Rev. Lett. **85**, 4940 (2000).
- <sup>13</sup> M. Covington *et al.*, Phys. Rev. Lett. **79**, 277 (1997); N.-C. Yeh *et al.*, *ibid.* **87**, 087003 (2001).
- <sup>14</sup> Y. Dagan and G. Deutscher, Phys. Rev. Lett. **87**, 177004 (2001).
- <sup>15</sup> R. Gonnelli *et al.*, Eur. Phys. J. B (Rapid Notes) **22**, 411 (2001).
- <sup>16</sup> D. Daghero, R.S. Gonnelli, G.A. Ummarino, and V. A. Stepanov, cond-mat/0207411.
- <sup>17</sup> C.R. Hu, Phys. Rev. Lett. **72**, 1526 (1994); S. Kashiwaya *et al.*, Phys. Rev. B **51**, 1350 (1995).
- <sup>18</sup> M. Fogelström, D. Rainer, J. A. Sauls, Phys. Rev. Lett. **79**, 281 (1997); Y. Tanuma, Y. Tanaka, and S. Kashiwaya, Phys. Rev. B **64**, 214519 (2001).
- <sup>19</sup> S. Sachdev, *e.print* cond-mat/0109419.
- <sup>20</sup> H. Ghosh, Phys. Rev. B **59**, 3357 (1999).
- <sup>21</sup> F. Wenger and S. Östlund, Phys. Rev. B **47**, 5977 (1993).
- <sup>22</sup> O.K. Andersen *et al.*, J. Phys. Chem. Solids **56**, 1573 (1995).
- <sup>23</sup> R. S. Markiewicz, Physica C **228**, 227 (1994).
- <sup>24</sup> In light of this discussion, we can understand the large values of the critical secondary coupling ( $V^{cr} > V_1$ ) obtained in Ref.<sup>20</sup> as due to the weak-coupling regime in which all the calculations are done.
- <sup>25</sup> This value of  $\omega_0$  corresponds the typical energy of the longitudinal optical phonons, which are strongly coupled to the electrons. Within the stripe-QCP scenario, it represents an estimate of the characteristic energy scale of the pairing interaction [see S. Andergassen *et al.*, Phys. Rev. Lett. **87**, 056401 (2001), and references therein.]
- <sup>26</sup> We emphasize here that the QCP we are referring to is responsible for the fluctuations mediating pairing, and it is different from the possible  $d_{x^2-y^2} \rightarrow d_{x^2-y^2} + id_{xy}$  QCP. In particular it does not (necessarily) involve time-reversal symmetry breaking.
- <sup>27</sup> D. L. Feng *et al.*, Phys. Rev. Lett. **86**, 5550 (2001); Y.-D. Chuang *et al.*, Phys. Rev. Lett. **87**, 117002 (2001); A. A. Kordyuk *et al.*, Phys. Rev. Lett. **89**, 077003 (2002).
- <sup>28</sup> V. I. Anisimov *et al.*, Phys. Rev. B **66**, 100502 (2002).
- <sup>29</sup> C. M. Varma, Phys. Rev. B **55**, 14554 (1997), and references therein.
- <sup>30</sup> C. Castellani, C. Di Castro, and M. Grilli, Phys. Rev. Lett. **75**, 4650 (1995).
- <sup>31</sup> P. Monthoux, A. V. Balatsky, and D. Pines, Phys. Rev. Lett. **67**, 3448 (1991); S. Sachdev and J. Ye, Phys. Rev. Lett. **69**, 2411 (1992);
- <sup>32</sup> A. Perali *et al.*, Phys. Rev. B **54**, 16216 (1996).
- <sup>33</sup> The two dimensionless functions are equal to  $\alpha_1(\kappa^2) = \sum_{\mathbf{k}} \cos k_x / (\kappa^2 + 2(2 - \cos k_x - \cos k_y))$  and  $\alpha_2(\kappa^2) = \sum_{\mathbf{k}} \cos k_x \cos k_y / (\kappa^2 + 2(2 - \cos k_x - \cos k_y))$ .